A Combined Theoretical/Experimental Laboratory Study on Isopropyl Nitrate Pyrolysis

J. Bourgalais[1,*], N. Vin[1], O. Herbinet[1], H.-H. Carstensen[2,3], M. U. Azuelta[2], F. Battin-Leclerc[1]

[1]Reactions and Chemical Engineering Laboratory (LRGP), National Center for Scientific Research (CNRS)-Université de Lorraine (UL), Nancy, France

[2]Thermochemical Processes Group (GPT), Aragon Institute for Engineering Research (I3A), Universidad de Zaragoza, Spain

[3]Fundacion Agencia Aragonesa para la Investigacion y el Desarrollo (ARAID), Zagaroza, Spain

Abstract

While the thermal decomposition of alkyl nitrates is dominated by the homolytic cleavage of the nitrate bond, the subsequent chemistry of the initial products is less well known. This work aims to improve the knowledge of alkyl nitrates kinetics by studying the pyrolysis of isopropyl nitrate (iPN) in a tubular reactor at atmospheric pressure and temperatures ranging from 373 to 773K and residence times of 2 s. Preliminary results show that iPN decomposition starts at 450 K with O-N bond fission producing isopropoxy radical (i-C_3H_7O) and NO_2. i-C_3H_7O is rapidly converted to acetaldehyde (CH_3CHO), which is the most abundant product detected. Other major products are formaldehyde (CH_2O), methanol (CH_3OH), nitromethane (CH_3NO_2), NO, methane, formamide ($CHONH_2$), and methyl nitrite (CH_3ONO). A modified POLIMI mechanism is able to predict the decomposition of iPN as well as some major product reasonably well but deviations for other species indicate that further improvements are needed.

Introduction

Isopropyl nitrate ($(CH_3)_2CHONO_2$, iPN) is an organic nitrate used as a fuel additive in gas turbine engines and in blends with diesel due to its high energy content, high density and the presence of three oxygen atoms which contribute to improve fuel performance. iPN is a promising "green" monopropellant which creates a high amount of thrust and can be used for a wide range of applications (e.g. space and aerial vehicles, underwater power sources, robotic actuators). iPN has many economic, health and technical advantages over conventional monopropellant engines such as hydrazine (N_2H_4) and its derivatives as it is non-toxic and non-corrosive, can be produced at low cost and has low susceptibility towards premature detonation.

Previous experimental studies on the thermal decomposition of iPN include shock tubes [1-5], rapid compression machines [6,7], flow and closed cells [4,8-11], and flames [12] completed by theoretical investigations [5]. These experiments conducted over a wide range of temperatures, pressures and compositions demonstrated that, like other organic nitrate [13], the thermal decomposition of iPN proceeds by a well-known radical mechanism. The initial dissociation of the nitrate bond leads to the formation of NO_2 and an alkoxy radical, isopropoxy (i-C_3H_7O) in the case of iPN.

While the initiation step is well established, the subsequent reactions leading to the observed final products are less well understood. Although an alkoxy radical can undergo a number of competing reactions pathways, the isopropoxy radical is expected to mainly decompose rapidly to form a methyl radical CH_3 and the carbonyl compound acetaldehyde (CH_3CHO) [11]. Thus, the observed species distribution depends on the subsequent interactions of iPN, acetaldehyde, methyl and NO_2. For example, methyl radicals and acetaldehyde, by reaction with NO_2, lead to the formation of many of the observed products such as nitromethane (CH_3NO_2), NO, formaldehyde (CH_2O), methanol (CH_3OH), water, CO_2 and the correct prediction of those requires that all important reactions are identified and that accurate rate coefficients have been assigned.

This work presents an experimental study of the pyrolysis of the iPN in a tubular reactor at low temperatures and provides quantitative data of most product species. It constitutes the first study at atmospheric pressure in a flow tube, extending the existing literature database. The data will be used to guide the development of an iPN model, to identify remaining gaps of our understanding of nitrate pyrolysis chemistry, and to support the ongoing effort to develop reliable and comprehensive mechanisms for nitrogen fuels.

Experimental Setup

The experimental setup has already been described in detail recently for a study on the pyrolysis of nitromethane [14] and only a brief description with the specifics related to this work is given here. Experiments were carried out in a tubular reactor (TR) at a constant pressure of 1.07 bar, and an inlet iPN mole fraction of 0.01 (high dilution in helium). Helium (purity of 99.999%) and iPN (purity of 98%) were purchased from Messer and Sigma-Aldrich, respectively. Gas flow rates were controlled by mass flow controllers (0.5% uncertainty) and the liquid flow rate by a Coriolis flow controller. The TR is a 600 cm long alumina tube with an inner diameter of 20 mm (thus a volume of 294 cm^3) and an outer diameter of 25 mm heated by an electrical furnace from Vecstar. Actual axial temperature profiles along the TR were measured using a S-type thermocouple (with an accuracy of 0.5% for the

*Corresponding author: jeremy.bourgalais@univ-lorraine.fr

measured temperatures). At the operating conditions of this study, the reactor can be approximated as plug flow reactor (PFR) [15]. The evolution of the product mole fractions was measured over a temperature range from 373 to 773K. The residence time of the gas in the reactor was kept constant to about 2s at the set-point temperature in the central zone of the tube where the temperature is quasi constant. The relative uncertainty in the flow measurements is around 0.5% for each controller, so about $\pm$ 0.1s on the residence time. A heated transfer line maintained at 433K was used for sampling to avoid product condensation between the reactor outlet and the analytical devices. Species were sampled at the outlet and analyzed using gas chromatography and Fourier-Transform Infrared (FTIR) spectroscopy (10-meter path cell). A gas chromatograph equipped with six-port sampling and switching valve connected to a split injector, a Plot-Q capillary column, a thermal conductivity detector (TCD) and a flame ionization detector (FID) was used for the quantification of light products and the reactant [15]. Reaction products were identified with a gas chromatograph coupled to a quadrupole mass spectrometer. Response factors were determined by either injecting calibration mixtures or by using the effective carbon number method. Relative uncertainties in mole fractions are estimated to be less than 10%. A FTIR was used to identify and quantify CH_2O, CO, H_2O, HCN, NO, CO_2 and CH_3OH. FTIR calibrations were obtained by injecting standards. The relative uncertainties of the FTIR data are slightly higher than those obtained by GC since interferences may occur between bands of absorbing species.

Theoretical Calculations

The CBS-QB3 and G4 levels as implemented in the Gaussian G16 suite of programs [16] were used to calculate thermochemical parameters to update the iPN decomposition related chemistry of the POLIMI mechanism. Since the calculation method has been described before in detail [17] only details specific to iPN chemistry are given here. Electronic energies are converted with the atomization method to enthalpies of formation. Thermal entropy contributions, entropies and heat capacities are calculated with statistical mechanics using the harmonic oscillator-rigid rotor assumption except for internal rotations which are separately evaluated as one-dimensional internal rotors with effective rotational constants [18]. Systematic deviations between calculated and known enthalpies of formations are corrected by applying bond additive corrections leading to generally good agreements (within 1 kcal/mol) with entries in the ATcT [19]. Since the G4 results require less corrections, high pressure rate coefficients of important reactions were calculated with transition state information at this level. Eckart tunneling corrections are applied. The Multiwell program [20] was used to generate pressure-dependent rate expressions when needed. More details about individual reactions may be found as comments in the kinetic model or further below.

Kinetic Mechanism

The mechanism used to simulate the pyrolysis of iPN in TR is based on the POLIMI mechanism [21]. The core of the mechanism has recently been improved by adding the reactions of the H_2/O_2 system and the C_1/C_2 sub-mechanisms from Metcalfe et al. [22], C_3 from Burke et al. [23] and a sub-model for heavier fuels from Ranzi et al. [24]. To this mechanism, several reactions have been added based on theoretical calculations and literature.
Three unimolecular decomposition pathways with similar energy (between 41.4 and 43.1 kcal/mol at the G4 level) of the transition states exist for iPN:

iPN $\rightarrow$ C2COJ + NO_2

iPN $\rightarrow$ CC=C + $HONO_2$

iPN $\rightarrow$ C2C=O + HONO

Since the propene (CC=C) and acetone ($C_2C=O$) forming channels proceed through tight transition states, only the bond scission reaction forming isopropoxy radical and NO_2 is important. MultiWell was used to calculate the rate expression for these reactions, which are incorporated in PLOG format.

H abstraction reactions from iPN by H, CH_3, NO_2 and NO_3 have been calculated at the G4 level. The results are implemented as irreversible forward and reverse reactions to decouple this information from the thermodynamic data taken from POLIMI. H abstraction from iPN produces two different radicals, depending on the abstraction site. The radical produced by H abstraction from the tertiary site, $CH_3C{\cdot}(ONO_2)CH_3$ is not stable but immediately dissociates to acetone and NO_2, while H abstraction from the methyl group leads to ${\cdot}CH_2CH(ONO_2)CH_3$. Pressure-dependent rate coefficients for important reaction channels of latter radical have been determined. The most favorable channels are the β- scission reaction that produces propene and NO_3 and a cyclization reaction forming a 5-membered N- containing ring which ultimately dissociates to acetaldehyde, formaldehyde and NO. However, since the rate expressions for the H abstraction from the methyl group are slow, these reactions have been found to be not important.

Other updates of the POLIMI model include the unimolecular reactions of nitromethane to CH_3ONO, CH_2O + NO, and CH_2O + HNO. The kinetic parameters used are those proposed by Zhu et al. [25]. The unimolecular dissociation of CH_2NO_2 to CH_2O + NO has been added with kinetic parameters calculated by quantum computing methods. The HCO + HNO recombination to CH_2NO_2 has been added with the kinetic parameters taken equal to those proposed by Xu et al. [26]. Finally, the reaction CH_3CHO + CH_3O to CH_3OH + CH_3CO has been added with kinetic parameters estimated by analogy with the metathesis reactions of the methyl radical on acetaldehyde present in the POLIMI mechanism [21].

The kinetic parameters of some reactions of the POLIMI mechanism have been adjusted. The kinetic parameters of the POLIMI mechanism for the reaction of CH_3O + NO have been replaced by those of Atkinson et al. [27]. The pre-exponential factor for the reaction

between $CH_3 + NO_2$ has been multiplied by 5 and the one for the reaction $CH_3O + CH_3NO_2$ by 10. The kinetic parameters for the reaction $CH_3CHO + CH_3$ have been taken equal to those obtained by a fit of several sets of kinetic parameters from the literature [28-37] and the ones for the $CH_2O + CH_3O$ reaction to those proposed by Tsang et al. [38].

Results

The model proposed in this work has been tested against a large set of experimental data newly measured in the present work. In the figures shown below, the lines represent the simulation results using the kinetic model in its current state and symbols represent the experimental data. All simulations were performed using the openSMOKE software package [39].

Figure 1 shows the evolution of the conversion as a function of temperature and residence time. iPN begins to degrade at 423K and is fully consumed at 548K.

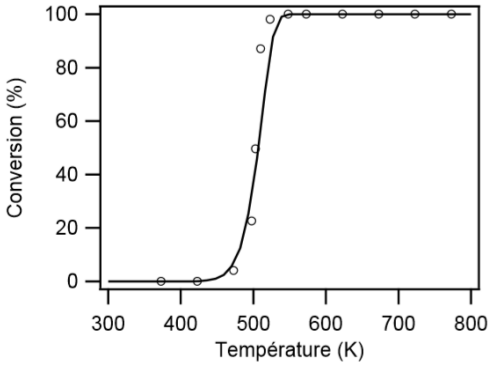

Figure 1. iPN conversion: comparison between experiment (open dots) and predictions (black line). Conditions: see text

The pyrolysis of isopropyl nitrate produces a large number of products. The main products are acetaldehyde, formaldehyde, methanol, nitromethane (CH_3NO_2), NO and methyl nitrite (CH_3ONO). Formamide ($HC(O)NH_2$) and CO are also detected with significant mole fractions as are acetone, isopropyl alcohol ($CH_3CH(OH)CH_3$), and methane. HCN, C_2H_4, methyl nitrate (CH_3ONO_2), and dimethylnitrosoamine ($(CH_3)_2N\text{-}NO$) have also been detected.

The majority of carbon and oxygen species has been properly quantified as the atomic balance presented in Figure 2 shows. The balance is calculated by the difference between the number of moles of the atomic element in the output stream divided by the number of moles of the atomic element in the input stream. The clear deviation of the nitrogen atom balance (>15%) is due to the fact that N_2 was not quantified in this study although it was identified in the GC-MS.

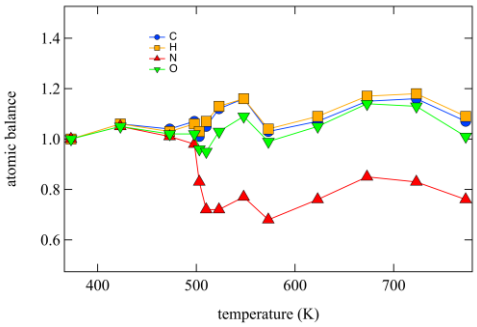

Figure 2. Atomic balance in C (blue dots), H (orange squares), N (red triangles), and O (down green triangles) during iPN pyrolysis for an inlet mole fraction of 0.01 and a residence time of 2s at atmospheric pressure.

The mole fraction profiles of the main products formed during iPN pyrolysis together with the predictions of the kinetic model are shown in Figure 3. Except for formaldehyde for which the mole fraction is underestimated by a factor of 3, and acetone, for which the model fails to reproduce its formation at low temperatures until it reaches a plateau value, the kinetic model reproduces the formation of both, major and minor species reasonably well. On the other hand, deviations of the model from the experimental results are more significant for the minor products except for propene. This indicates that the current model either lacks important reactions or that some rate expressions are severely inaccurate. Keeping in mind that iPN pyrolysis occurs at very low temperatures, hence conditions at which small uncertainties of activation energies have profound consequences on the rate coefficients, it becomes clear that the new experimental data present a stringent test for any kinetic model. The observed deviations clearly demonstrate the potential to improve our understanding of this chemistry.

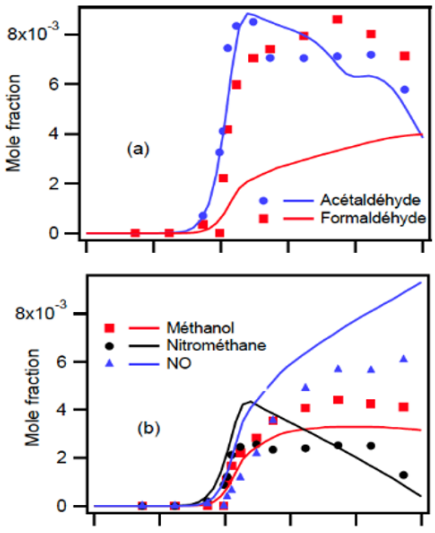

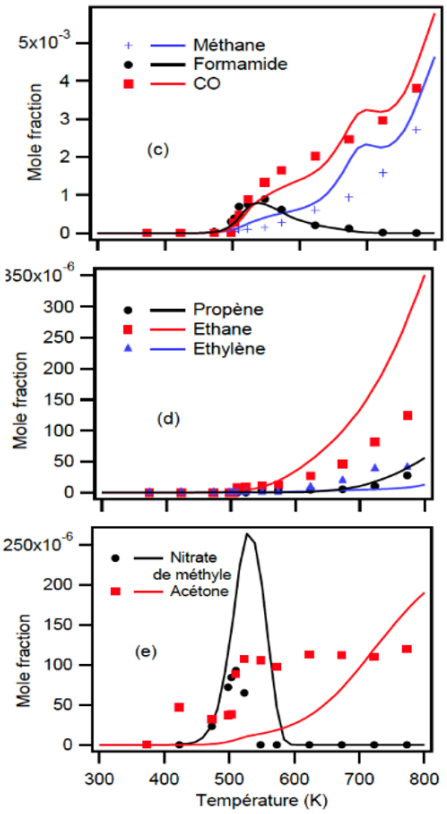

Figure 3. Comparison of experimental data and numerical model predictions on the evolution as a function of temperature of the mole fraction of (a) acetaldehyde/formaldehyde, (b) methanol/nitromethane, (c) methane/formamide/CO, (d) propene/ethane/ethylene, and (e) methyl nitrate/acetone during iPN pyrolysis for an inlet mole fraction of 0.01 and a residence time of 2s at atmospheric pressure. The symbols correspond to the experimental results and the curves to the predictions of the numerical model.

Discussion

To analyze the reaction pathways of iPN pyrolysis, a rate analysis performed with OpenSMOKE is shown in Figure 6. From this rate analysis, it is clear that the only route of decomposition of iPN at 550 K is the cleavage of the O-NO_2 bond (100%) as indicated by most previous studies in the literature.

The O-NO_2 breaking bond causes the formation of i-C_3H_7O radical and NO_2. The radical decomposes instantaneously by reaction of beta-scission into acetaldehyde and methyl radical. Acetaldehyde then reacts by H-abstraction reaction with CH_3O radical to form methanol and CH_3CO radical. The latter decomposes by reaction of alpha-scission to form CO and methyl radical. Note that the CO profile is reproduced quite well similar to the acetaldehyde profile. This indicates that this chemistry is likely well implemented in the kinetic model. Methyl radical can react with NO_2 to form nitromethane or to form CH_3O and NO radical. The branching ratio between latter two reactions is important because it will greatly influence the formation of nitromethane, NO and CH_3O radical. The CH_3O radical can abstract a H atom from nitromethane to form methanol and the nitromethyl radical that immediately decomposes to formaldehyde and NO. Even a factor of 10 increase of the literature value did not produce enough formaldehyde, though, to capture the high amounts observed in the experiment. To a lesser extent, CH_3O radical can also react with NO to form the HNO radical and formaldehyde. The formation of CH_3O radical is important here because it is involved in reactions leading to the formation of several major products such as methanol, formaldehyde and NO. The water formation pathway results from the reaction of HONO with itself, also forming NO and NO_2. HONO is formed in the reaction between NO_2 and HNO. Methane, not shown in Figure 4, is formed in H abstraction reactions of methyl radicals from acetaldehyde as well as HNO.

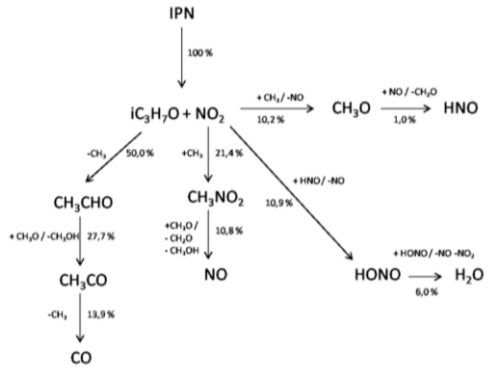

Figure 4. Simplified flow analysis carried out from the model developed for the pyrolysis of iPN for the consumption of the reactant in TR (550 K, mole fraction of iPN at the inlet of 0.01, residence time of 2 s, P=1.07 bar). The numbers on the arrows represent the consumption rate normalized by the total reagent consumption rate.

The formation of minor species is not presented in Figure 4 for clarity. Ethane is formed by a recombination of two methyl radicals. The formation of acetone is mainly due to the minor C-H beta-scission channel of i-C_3H_7O radical. Propene is formed by beta-scission of the iPN radical $CH_2CHCH_3ONO_2$, which is produced by H abstraction reactions. Note that both, acetone and propene are experimentally observed at much lower temperatures than predicted. A possible explanation for the deviation could be that the model underestimates the importance of H abstraction reactions from iPN. H abstraction from the CH3 groups would yield propene and that of the tertiary C-H would produce acetone. The kinetic model contains several H abstraction reactions with rate coefficients calculated as part of this work. These should be critically re-evaluated given the low temperatures of the experiments and the critical importance of the barrier heights as well as contributions from tunneling. Methyl nitrate results from the reaction between CH_3O and NO_2.

Conclusion

The study of the pyrolysis of iPN was carried out in a tubular reactor. The temperatures of the study were between 373 and 773 K. The residence time was set at 2 s with a mole fraction of 0.01 reactant. All experiments were carried out at a pressure of 1.07 bar. The following products were identified: acetaldehyde, formaldehyde, methane, CO, NO, methanol, nitromethane, NO_2, formamide, methyl nitrate, methyl nitrite, acetone, H_2O, CO_2, ethane, isopropyl alcohol, ethylene, propene and HCN. iPN is a very reactive molecule reacting from 423 K and up to 548 K, matching with a total consumption. The variety of detected products for such a small fuel highlighted the complexity of the thermal decomposition mechanism.

The analysis of the kinetic model developed in this study has enabled a better understanding of the decomposition reactions of iPN as well as the formation of the products obtained. The chemistry of iPN pyrolysis is thus better understood. The importance of the reaction of decomposition of iPN by the O-NO_2 breaking bond has been demonstrated by flow rate and sensitivity analysis of the kinetic model developed in this study.

Acetaldehyde is rather stable of the expected formation is seen and the decay is for a narrow window in which high CH_3 and CH_3O concentrations are predicted (not shown here). HCHO yields even higher but the kinetic model does not predict this. There is a potential missing reaction that converts CH_3NO_2 to HCHO due to its overestimation. CH_3ONO_2 is also overpredicted maybe because CH_3O is too stable and can react with NO_2. There is may also be a missing pathway from CH_3O towards HCHO.

In particular the large deviation between experimental and predicted formaldehyde yields suggest that some important reactions are missing in the current model. Current efforts try to address these deficiencies by (a) double-checking the kinetic parameters used in the current model and by looking for reaction pathways specific to nitrate chemistry that have been overlooked too far.

Acknowledgments

The experimental work on CH_3NO_2 pyrolysis has been supported by TERBIS, 943 rue Pasteur, 60700 Pont Sainte Maxence, France. MUA and HHC express their gratitude to Aragón Government and European Social Fund (GPT Group, I3A) and MCIU (project RTI2018-098856) for financial support.

References

[1] Jullien, J., Pechine, J. M., Perez, F., & Sadek, M. A. (1983). Décomposition thermique en phase gazeuse du nitrate d'isopropyle. *Propellants, Explosives, Pyrotechnics*, *8*(4), 99-101.

[2] Zaslonko, I. S., Smirnov, V. N., & Tereza, A. M. (1993). High-temperature decomposition of methyl, ethyl, and isopropyl nitrates in shock waves. *Kinetics and catalysis*, *34*(4), 531-538.

[3] Toland, A., & Simmie, J. M. (2003). Ignition of alkyl nitrate/oxygen/argon mixtures in shock waves and comparisons with alkanes and amines. *Combustion and flame*, *132*(3), 556-564.

[4] Borisov, A. A., Troshin, K. Y., & Mikhalkin, V. N. (2016). Ignition and combustion of isopropyl nitrate. *Russian Journal of Physical Chemistry B*, *10*(5), 780-784.

[5] Fuller, M. E., & Goldsmith, C. F. (2019). Shock Tube Laser Schlieren Study of the Pyrolysis of Isopropyl Nitrate. *The Journal of Physical Chemistry A*, *123*(28), 5866-5876.

[6] Beeley, P., Griffiths, J. F., & Gray, P. (1980). Rapid compression studies on spontaneous ignition of isopropyl nitrate art I: Nonexplosive decomposition, explosive oxidation and conditions for safe handling. *Combustion and flame*, *39*(3), 255-268.

[7] Beeley, P., Griffiths, J. F., & Gray, P. (1980). Rapid compression studies on spontaneous ignition of isopropyl nitrate Part II: Rapid sampling, intermediate stages and reaction mechanisms. *Combustion and Flame*, *39*(3), 269-281.

[8] Griffiths, J. F., Gilligan, M. F., & Gray, P. (1975). Pyrolysis of isopropyl nitrate. I. Decomposition at low temperatures and pressures. *Combustion and Flame*, *24*, 11-19.

[9] Griffiths, J. F., Gilligan, M. F., & Gray, P. (1976). Pyrolysis of isopropyl nitrate—II. Decomposition at high temperatures and pressures. *Combustion and Flame*, *26*, 385-393.

[10] Hansson, T., Pettersson, J. B., & Holmlid, L. (1989). A molecular beam mass-spectrometric study of isopropyl nitrate pyrolysis reactions at short residence times and temperatures up to 700 K. *Journal of the Chemical Society, Faraday Transactions 2: Molecular and Chemical Physics*, *85*(9), 1413-1423.

[11] Morin, J., & Bedjanian, Y. (2016). Thermal decomposition of isopropyl nitrate: kinetics and products. *The Journal of Physical Chemistry A*, *120*(41), 8037-8043.

[12] Powling, J., & Smith, W. A. W. (1957). Flame decomposition of the propyl nitrates. *Combustion and Flame*, *1*(3), 308-320.

[13] Phillips, L. (1947). Thermal decomposition of organic nitrates. *Nature*, *160*(4074), 753-754.

[14] Shrestha, K. P., Vin, N., Herbinet, O., Seidel, L., Battin-Leclerc, F., Zeuch, T., & Mauss, F. (2020). Insights into nitromethane combustion from detailed kinetic modeling–Pyrolysis experiments in jet-stirred and flow reactors. *Fuel*, *261*, 116349.

[15] Vin, N., Battin-Leclerc, F., & Herbinet, O. (2018). A study of thermal decomposition of bromoethane. *Journal of Analytical and Applied Pyrolysis*, *136*, 199-207.

[16] Frisch, M. J., Trucks, G. W., Schlegel, H. B., Scuseria, G. E., Robb, M. A., Cheeseman, J. R., ... & Fox, D. J. (2016). Gaussian 16, revision C. 01.

[17] Ince, A., Carstensen, H. H., Reyniers, M. F., & Marin, G. B. (2015). First-principles based group additivity values for thermochemical properties of

substituted aromatic compounds. *AIChE Journal*, *61*(11), 3858-3870.
[18] East, A. L., & Radom, L. (1997). Ab initio statistical thermodynamical models for the computation of third-law entropies. *The Journal of chemical physics*, *106*(16), 6655-6674.
[19] B. Ruscic and D. H. Bross, Active Thermochemical Tables (ATcT) values based on ver. 1.122o of the Thermochemical Network (2020); available at ATcT.anl.gov
[20] Barker, J. R., Nguyen, T. L., Stanton, J. F., Aieta, C., Ceotto, M., Gabas, F., ... & Stimac, P. J. (2016). MultiWell-2017 Software Suite; JR Barker, University of Michigan. *Ann Arbor, Michigan, USA*.
[21] Ranzi, E., Frassoldati, A., Grana, R., Cuoci, A., Faravelli, T., Kelley, A. P., & Law, C. K. (2012). Hierarchical and comparative kinetic modeling of laminar flame speeds of hydrocarbon and oxygenated fuels. *Progress in Energy and Combustion Science*, *38*(4), 468-501.
[22] Metcalfe, W. K., Burke, S. M., Ahmed, S. S., & Curran, H. J. (2013). A hierarchical and comparative kinetic modeling study of C1− C2 hydrocarbon and oxygenated fuels. *International Journal of Chemical Kinetics*, *45*(10), 638-675.
[23] Burke, S. M., Burke, U., Mc Donagh, R., Mathieu, O., Osorio, I., Keesee, C., ... & Curran, H. J. (2015). An experimental and modeling study of propene oxidation. Part 2: Ignition delay time and flame speed measurements. *Combustion and Flame*, *162*(2), 296-314.
[24] Ranzi, E., Frassoldati, A., Stagni, A., Pelucchi, M., Cuoci, A., & Faravelli, T. (2014). Reduced kinetic schemes of complex reaction systems: fossil and biomass-derived transportation fuels. *International Journal of Chemical Kinetics*, *46*(9), 512-542..
[25] Zhu, R. S., Raghunath, P., & Lin, M. C. (2013). Effect of roaming transition states upon product branching in the thermal decomposition of CH3NO2. *The Journal of Physical Chemistry A*, *117*(32), 7308-7313.

[26] Xu, Z. F., & Lin, M. C. (2004). A Computational Study of the Kinetics and Mechanism for the Reaction of HCO with HNO. *International journal of chemical kinetics*, *36*(4), 205-215.
[27] Atkinson, R., Baulch, D. L., Cox, R. A., Hampson Jr, R. F., Kerr, J. A., Rossi, M. J., & Troe, J. (1997). Evaluated kinetic, photochemical and heterogeneous data for atmospheric chemistry: Supplement V. IUPAC Subcommittee on Gas Kinetic Data Evaluation for Atmospheric Chemistry. *Journal of Physical and Chemical Reference Data*, *26*(3), 521-1011.
[28] Laidler, K. J., & Liu, M. T. H. (1967). The mechanism of the acetaldehyde pyrolysis. *Proceedings of the Royal Society of London. Series A. Mathematical and Physical Sciences*, *297*(1450), 365-375.
[29] Brinton, R. K., & Volman, D. H. (1952). Induced Decomposition of Acetaldehyde by Radicals. *The Journal of Chemical Physics*, *20*(6), 1053-1054.
[30] Volman, D. H., & Brinton, R. K. (1952). Reactions of Free Radicals with Aldehydes. The Reactions of Methyl and t-Butoxy Radicals with Acetaldehyde and Acrolein. *The Journal of Chemical Physics*, *20*(11), 1764-1768.
[31] Dodd, R. E. (1955). The Reaction of Methyl Radicals with Acetaldehyde. *Canadian Journal of Chemistry*, *33*(4), 699-704.
[32] Birrell, R. N., & Trotman-Dickenson, A. F. (1960). 417. The reactions of alkyl radicals. Part VI. The reactions of methyl radicals with aliphatic aldehydes. *Journal of the Chemical Society (Resumed)*, 2059-2063.
[33] Kerr, J. A., & Calvert, J. G. (1965). The Formation and Decomposition Reactions of the Acetyle Radical and the Heat of Formation of the Acetyl Radical. *The Journal of Physical Chemistry*, *69*(3), 1022-1029.
[34] Liu, M. T., & Laidler, K. J. (1968). Elementary processes in the acetaldehyde pyrolysis. *Canadian Journal of Chemistry*, *46*(4), 479-490.
[35] Baldwin, R. R., Langford, D. H., Matchan, M. J., Walker, R. W., & Yorke, D. A. (1971, January). The high-temperature oxidation of aldehydes. In *Symposium (International) on Combustion* (Vol. 13, No. 1, pp. 251-259). Elsevier.
[36] Warnatz, J. (1984). Rate coefficients in the C/H/O system. In *Combustion chemistry* (pp. 197-360). Springer, New York, NY.
[37] Baulch, D. L., Cobos, C. J., Cox, R. A., Frank, P., Hayman, G., Just, T., ... & Warnatz, J. (1994). Evaluated kinetic data for combustion modeling. Supplement I. *Journal of Physical and Chemical Reference Data*, *23*(6), 847-848.
[38] Tsang, W., & Hampson, R. F. (1986). Chemical kinetic data base for combustion chemistry. Part I. Methane and related compounds. *Journal of physical and chemical reference data*, *15*(3), 1087-1279.
[39] Cuoci, A., Frassoldati, A., Faravelli, T., & Ranzi, E. (2015). OpenSMOKE++: An object-oriented framework for the numerical modeling of reactive systems with detailed kinetic mechanisms. *Computer Physics Communications*, *192*, 237-264.